Elektrotech. Inftech. (2023) 140:497–516
https://doi.org/10.1007/s00502-023-01148-y

e+i elektrotechnik und informationstechnik

Lumped model eddy current analysis of influence factors on PM segmentation effectiveness

Mike Königs · Bernd Löhlein

Received: 6 November 2022 / Accepted: 31 January 2023 / Published online: 4 August 2023

Abstract This is the second of a series of papers on new methods for the calculation of eddy current losses in permanent magnets (PMs) and the shortcomings of previous analyses. Our first paper extended Ruoho's work on harmonic field distributions to the reaction field of eddy currents within permanent magnets. The approach was based on the methods of the harmonic complex AC calculation. In this paper, the models presented in our previous paper are further extended to allow a harmonic calculation of eddy current losses in permanent magnets for homogeneous fields, including the effects of eddy current losses in an adjacent ferromagnetic material, leakage flux factors, and non-constant inductance.

Keywords Permanent magnet · Eddy current · Eddy current losses · Segmentation · High-speed drives · Inverter-related losses

Analyse von Einflussfaktoren auf PM-Segmentierungseffizienz anhand eines Modells mit konzentrierten Ersatzelementen

Zusammenfassung In der zweiten Veröffentlichung dieser Reihe werden Einflussfaktoren auf Segmentierungseffektivitäten untersucht. Dazu werden die Ergebnisse der ersten Veröffentlichung nochmals erweitert, um Wirbelstromverluste in umgebenden Ferromagnetika, die Luftspaltweite, das Streuverhalten und nichtkonstante Induktivitäten zu berücksichtigen. Das Verfahren basiert auf den Methoden der komplexen Wechselstromtechnik. Unter Berücksichtigung der Einflussfaktoren lassen sich Aussagen über die Validität bisheriger Berechnungsmethodiken treffen.

Schlüsselwörter Permanentmagnet · Wirbelstrom · Wirbelstromverluste · Segmentierung · Hochdrehzahlantriebe · Umrichterbedingte Verluste

Abbreviations

B	Magnetic flux density
EC	Eddy current
I	Electrical current
j	Imaginary unit
K_σ	Leakage flux factor. Additional leakage inductance as a percentage of the main inductance
l	Geometric lenght
l_1	Geometric lenght of a magnet
l_σ	Air gap width
L	Inductance
N	Number of discrete eddy current paths
P	Active power
PM	Permanent magnet
R	Resistance
V	Electrical voltage
X	Reactance
x	Geometric integration variable
μ_0	Permeability of the vacuum
μ_r	Relative material permeability
ρ	Specific resistance
$\mathcal{M}$	System matrix
ω	Angular frequency

1 Introduction

Inverter related losses are a major contributor to eddy current losses in the permanent magnets of permanent magnet synchronous machines (PMSM). Inverter related losses are rarely considered in finite element

M. Königs · B. Löhlein (✉)
Institute for Innovative Drive Technology,
University of Applied Sciences Flensburg,
Kanzleistr. 91–93, 24943 Flensburg, Germany
bernd.loehlein@hs-flensburg.de

method (FEM) simulations for drive design. This is mainly due to the increased complexity and computational time required to set up time steps for inverter switching frequencies and spatial harmonics due to stator slotting instead of just the fundamental frequency of the drive. However, with recommended inverter switching frequencies of at least 10 times the fundamental frequency of the drive, this results in a tenfold increase in computation time in the worst case. In addition, simple models for estimating the current ripple for current injection may not be accurate enough since eddy current losses in the machine are the cause of non-constant inductance behavior. A strong direct coupling between the simulated inverter and the simulated drive would be highly desirable but has its own drawbacks in terms of computation time. Based on analytical models a computation of the inverter related losses could be feasible. In this work, the previously described model [7] extended to a harmonic voltage based solution. Not only the excitation coil with leakage and main inductance is modeled, but also a simplified model for the adjacent system eddy current losses is introduced. It will be investigated whether the current literature approach of calculating the magnetic fields in the machine and separating the field calculation from the loss calculation is acceptable. It is hypothesized that at high frequencies there is a strong coupling between hysteresis and eddy current losses in the ferromagnetic material surrounding the magnet and the eddy current losses in the magnet itselv. Although hysteresis effects are expected to be a major contributor to the loss characteristics of eddy current losses in PM their effects are not yet considered in this paper.

2 Harmonic coil based calculations of eddy current losses

The harmonic calculations of eddy current losses in permanent magnets are based on the models developed in the first paper in this series [7]. While Ruoho [1] uses eddy current path resistances for an electrostatic solution, the model in [7] introduces self- and mutual-inductance for each eddy current path. This allows the consideration of eddy current reaction fields. For single harmonics the methods of complex AC calculations using reactance calculations can be used even when introducing models for adjacent eddy current losses and coil behavior. A simple yoke geometry with an excitation coil is used to model the system behavior. Fig. 1 shows a section of the geometric design.

Fig. 2 shows the electrical equivalent circuit including a model for eddy current losses in a ferromagnetic material. Both the eddy current losses in the ferromagnetic material and the hysteresis of the material have nonlinear damping characteristics on the magnetic fields and are expected to affect the effectiveness of magnet segmentation methods.

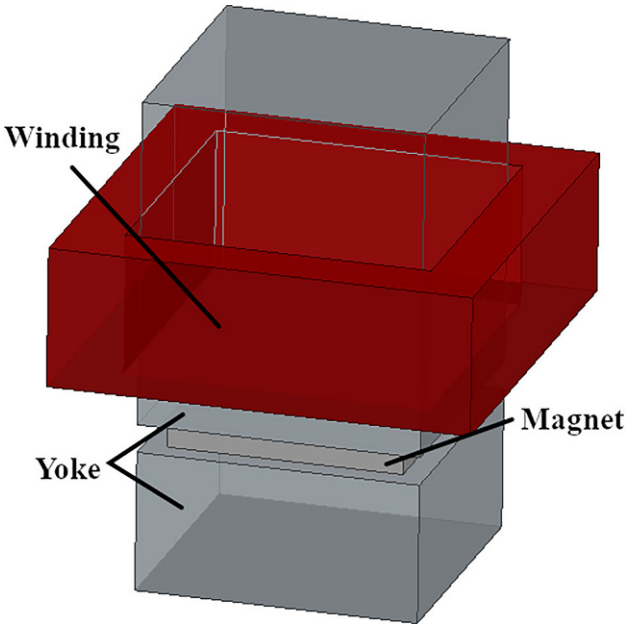

Fig. 1 Geometric design of the assumed model

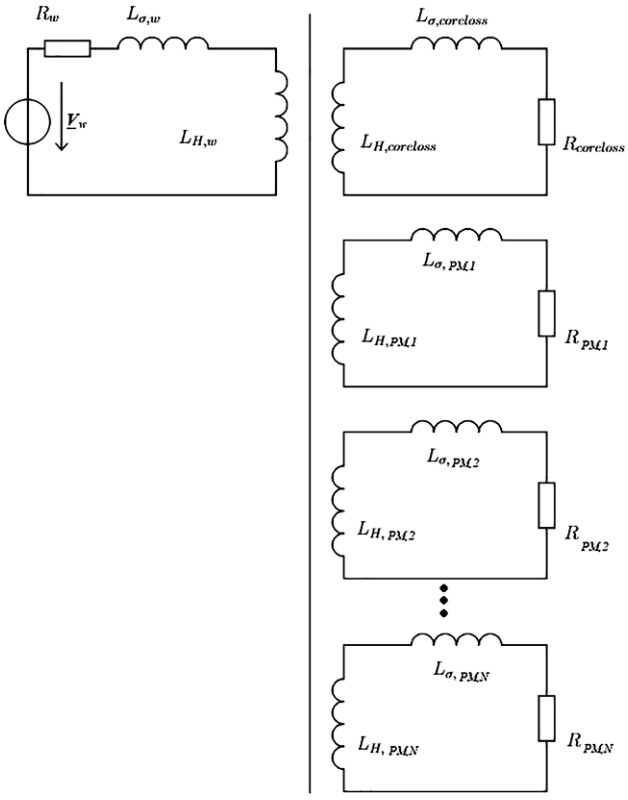

Fig. 2 Equivalent electrical circuit

The lumped circuit elements are schematically added to the geometry in Fig. 3. Each circuit path consists of two inductances and one ohmic resistance. As can be seen in Fig. 3, the magnet is divided

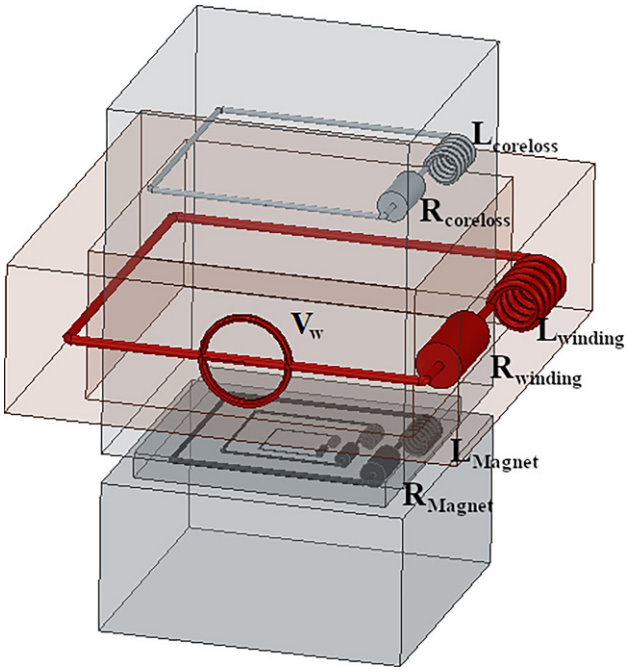

Fig. 3 Schematic electrical lumped parameter circuits

into a large number of sub-circuits, which allows the effects of current displacement to be taken into account. The parameters of the lumped resistances and inductances for a discrete number of eddy current paths can be calculated in the same way as in [7]. The path model is shown in Fig. 4. The given model lacks consideration of current displacement effects in the eddy current loss model of the ferromagnetic yoke. This is true under the assumption that the width of the electrical sheet metal commonly used for ferromagnetic yokes is significantly smaller than the theoretical skin depth for the given frequencies and materials.

Based on the lumped element model, the system equations can be formulated using the complex AC calculation methods. The formula is given in

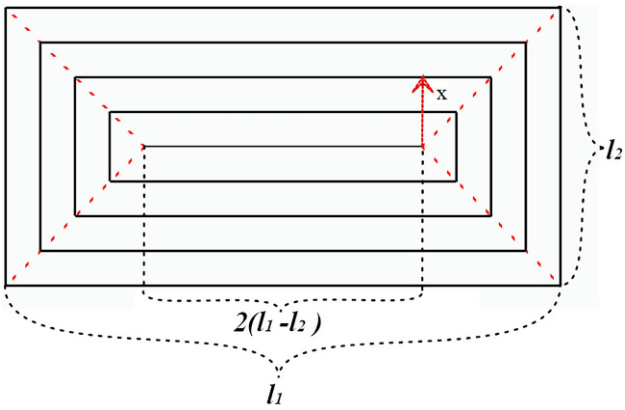

Fig. 4 Eddy current path model

Eq. (1). The equations for the element calculation are given in [7].

$$\begin{pmatrix} \underline{V}_w \\ \underline{V}_{\text{coreloss}} \\ \underline{V}_{\text{PM},1} \\ \vdots \\ \underline{V}_{\text{PM},N} \end{pmatrix} = \begin{pmatrix} R_w + j \cdot X_w & j \cdot X_{\text{EC},w} & j \cdot X_{\text{PM1},w} & \cdots & j \cdot X_{\text{PM}N,w} \\ j \cdot X_{w,\text{EC}} & R_{\text{coreloss}} + j \cdot X_{\text{EC}} & j \cdot X_{\text{PM1,EC}} & \cdots & j \cdot X_{\text{PM}N,\text{EC}} \\ j \cdot X_{w,M1} & j \cdot X_{\text{EC,PM1}} & R_{\text{PM1}} + j \cdot X_{\text{PM1}} & & j \cdot X_{\text{PM}N,\text{PM1}} \\ & \vdots & & & \\ j \cdot X_{w,\text{PM}N} & j \cdot X_{\text{EC,PM}N} & j \cdot X_{\text{PM1,PM}N} & & R_{\text{PM}N} + j \cdot X_{\text{PM}N} \end{pmatrix} \cdot \begin{pmatrix} \underline{I}_w \\ \underline{I}_{\text{coreloss}} \\ \underline{I}_{\text{PM},1} \\ \vdots \\ \underline{I}_{\text{PM},N} \end{pmatrix} \quad (1)$$

Only the excitation coil is subject to an external voltage source, which can be replaced by a current source. The voltages of the other partial circuits can be set to zero.

Table 1 Parameters of the base model

Magnet geometry	Height	Width	Depth
	5 mm	50 mm	50 mm
Relative permeability magnet μ_r	1.04		
Resistivity magnet ρ_{NdFeB}	$1.6\,\mu\Omega\mathrm{m}^{-1}$		
Yoke geometry	Height	Width	Depth
	200 mm	50 mm	50 mm
Relative permeability yoke μ_r	2000		
Air gap width l_δ	1 mm		
Coil resistance	$0.1\,\Omega$		
Coil number of turns	20		
Coil voltage	10 V		
Effective yoke EC resistance	$1000\,\Omega$		
Coil leakage flux $K_{\sigma,\mathrm{coil}}$	150 %		
Core leakage flux $K_{\sigma,\mathrm{core}}$	0 %		
Magnet leakage flux $K_{\sigma,\mathrm{magnet}}$	0 %		
Choke inductance L_{choke}	0 H		

$$\begin{pmatrix} \underline{V}_w \\ 0\,\mathrm{V} \\ 0\,\mathrm{V} \\ \vdots \\ 0\,\mathrm{V} \end{pmatrix} = \begin{pmatrix} R_w + j\cdot X_w & j\cdot X_{\mathrm{EC},w} & j\cdot X_{\mathrm{PM1},w} & \cdots & j\cdot X_{\mathrm{PM}N,w} \\ j\cdot X_{w,\mathrm{EC}} & R_{\mathrm{coreloss}} + j\cdot X_{\mathrm{EC}} & j\cdot X_{\mathrm{PM1,EC}} & \cdots & j\cdot X_{\mathrm{PM}N,\mathrm{EC}} \\ j\cdot X_{w,\mathrm{PM1}} & j\cdot X_{\mathrm{EC,PM1}} & R_{\mathrm{PM1}} + j\cdot X_{\mathrm{PM1}} & \cdots & j\cdot X_{\mathrm{PM}N,\mathrm{PM1}} \\ \vdots & \vdots & \vdots & & \vdots \\ j\cdot X_{w,\mathrm{PM}N} & j\cdot X_{\mathrm{EC,PM}N} & j\cdot X_{\mathrm{PM1,PM}N} & \cdots & R_{\mathrm{PM}N} + j\cdot X_{\mathrm{PM}N} \end{pmatrix} \cdot \begin{pmatrix} \underline{I}_w \\ \underline{I}_{\mathrm{coreloss}} \\ \underline{I}_{\mathrm{PM},1} \\ \vdots \\ \underline{I}_{\mathrm{PM},N} \end{pmatrix} \tag{2}$$

The currents can be obtained by inverting the system matrix $\underline{\mathscr{M}}$.

$$\vec{\underline{I}} = \underline{\mathscr{M}}^{-1} \cdot \vec{\underline{V}} \tag{3}$$

The total PM eddy current losses are then calculated by adding the sub-circuit losses of each PM eddy current path.

$$P_{\mathrm{eddy,Magnet}} = \sum_{n=1}^{N} |\underline{I}_{\mathrm{Magnet,n}}|^2 \cdot R_{M,n} \tag{4}$$

3 Model verification

The analytical base model has been verified against a FEM analysis in previous publications [7]. The analysis in the previous work was limited to a flux impressed analysis where the total external magnetic flux remains constant, which agrees quite well with the results for current impressed analyses. This work extends the model to voltage impressed analysis, therefore a model verification based on a voltage impressed harmonic FEM analysis is performed. The geometry used in the FEM analysis is shown in Fig. 5. Table 1 list the parameters used in the analytical verification.

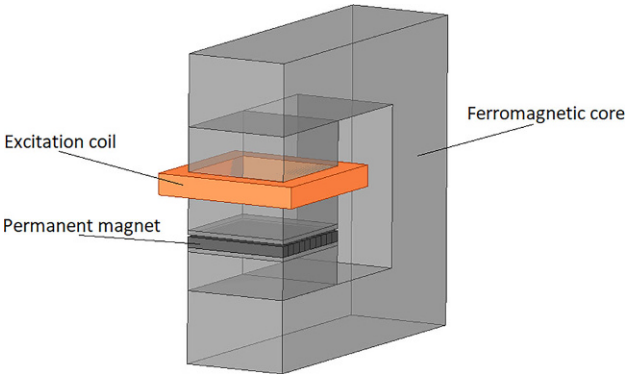

Fig. 5 Geometry of the FEM model

Fig. 6 shows the eddy current losses for various frequencies and segmentations for both the FEM analysis and the analytical analysis. The number of turns is 20 and the impressed voltage is 10 V. The comparisons of the model with the current impressed analysis are given in [7]. The FEM analysis is performed in Ansys Maxwell 2021 R2. The results of the analytical tool agree well with the results of the FEM analysis. For small number of segments ($N = 1$) and large frequencies ($f = 20\,\mathrm{kHz}$) the relative deviation is 34%. This is the largest deviation in the set. For larger number of segments the deviation is much lower (22% for $N = 2$, 2.2% for $N = 5$, 3.8% for $N = 10$). It should be noted, that the sensitivity to the flux leakage factors is high. While the FEM analysis gives the correct value for the leakage flux, the analytical analysis requires an estimation of the leakage flux or an initial calibration.

4 Factors of influence on PM eddy current losses

The simple model given in section II. allows the evaluation of factors affecting permanent magnet (PM) eddy current losses. A base model is subject to variation. The parameters of the base model are given in Table 2.

Three base cases are relevant for a parameter analysis.

1. **Flux impressed analysis:**
   This model was used in [7] and will not be discussed further in this paper. Furthermore, established analysis models use this analysis setup [2–5].

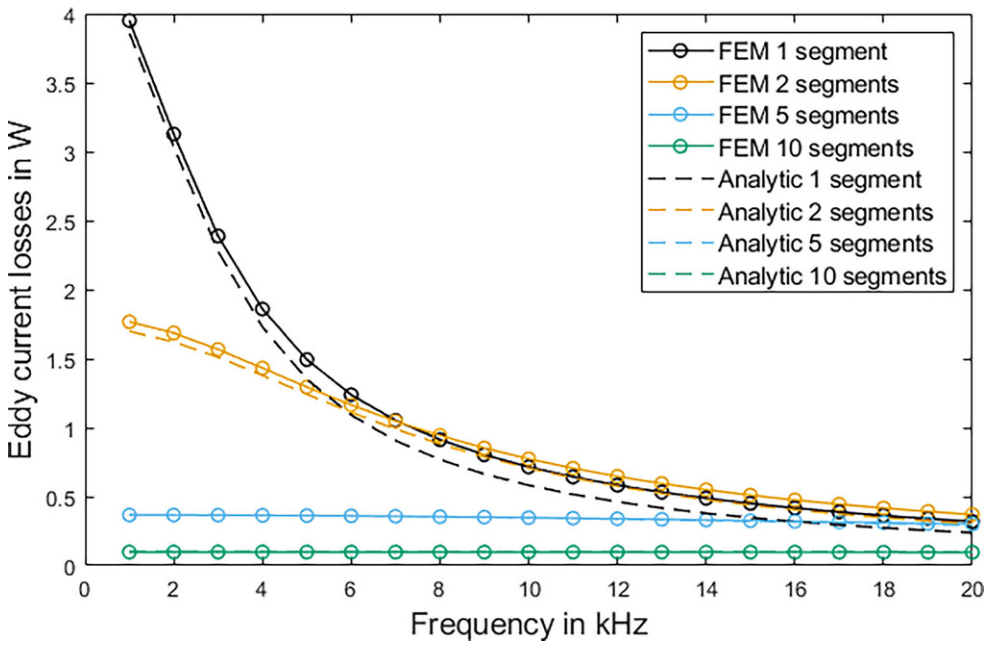

Fig. 6 Eddy current losses for various frequencies and segmentation numbers obtained by analytical analysis and FEM analysis

Table 2 Parameters of the base model

Magnet geometry	Height	Width	Depth
	5 mm	50 mm	50 mm
Relative permeability magnet μ_r	1.04		
Resistivity magnet ρ_{NdFeB}	$1.6\,\mu\Omega\text{m}^{-1}$		
Yoke geometry	Height	Width	Depth
	100 mm	50 mm	50 mm
Relative permeability yoke μ_r	4000		
Airgapwidth l_δ	1 mm		
Coil resistance	$1\,\Omega$		
Coil number of turns	40		
Coil voltage	1 V		
Excitation frequency	8000 Hz		
Effective yoke EC resistance	$1\,\Omega$		
Coil leakage flux $K_{\sigma,\text{coil}}$	10 %		
Core leakage flux $K_{\sigma,\text{core}}$	10 %		
Magnet leakage flux $K_{\sigma,\text{magnet}}$	10 %		
Choke inductance L_{choke}	0 H		

2. **Current impressed analysis:**
   The current impressed analysis is the analysis closest to previous work where the source flux distribution is calculated by FEM analysis and then the eddy current distribution is then calculated, e.g. by the method of images [4, 5]. This analysis should be valid for winding harmonics where the coil current is controlled by the PI controller of the inverter.

3. **Voltage impressed analysis:**
   The voltage impressed analysis is better suited for segmentation effects on inverter related losses. Since most inverters use intermediate voltage circuits, the current amplitudes will differ for various non-constant inductances.

In the following chapters, cases (2) and (3) will be analyzed in more detail.

4.1 Current impressed analysis

First, the evaluation of the influencing factors on PM eddy current losses for the current impressed analysis is given. The best known factor affecting eddy current losses in permanent magnets is the frequency of the magnetic flux. In the case of a current impressed analysis with constant excitation current, as shown in Fig. 7, the eddy current losses within the PM increase for any number of segments. It is noteworthy is that, due to the reaction flux, the losses do not increase with the square of the frequency, as [6] would suggest at first glance. For low frequencies, it can be observed that segmentation can reduce the eddy current losses for homogeneous fields even for a small number of segments. As the frequency increases, a maximum loss segmentation can be observed. The maximum loss segmentation number increases as the flux frequency increases. This phenomenon can also be attributed to the reaction flux. At high frequencies, the low eddy current resistance of unsegmented magnets hardly limits the currents and allows for a large compensation of the magnetic flux.

As noted, the reaction flux can alter the eddy current losses in the PM. Therefore, it is important to investigate factors that can manipulate the reaction flux behavior. One such factor is the air gap width. Fig. 8 shows the eddy current losses in the example permanent magnet for various air gap widths and segmentation numbers. A larger air gap inhibits the formation of the reaction flux. As a direct result, lower segmentation numbers are required to effectively reduce eddy current losses. Due to the increased overall

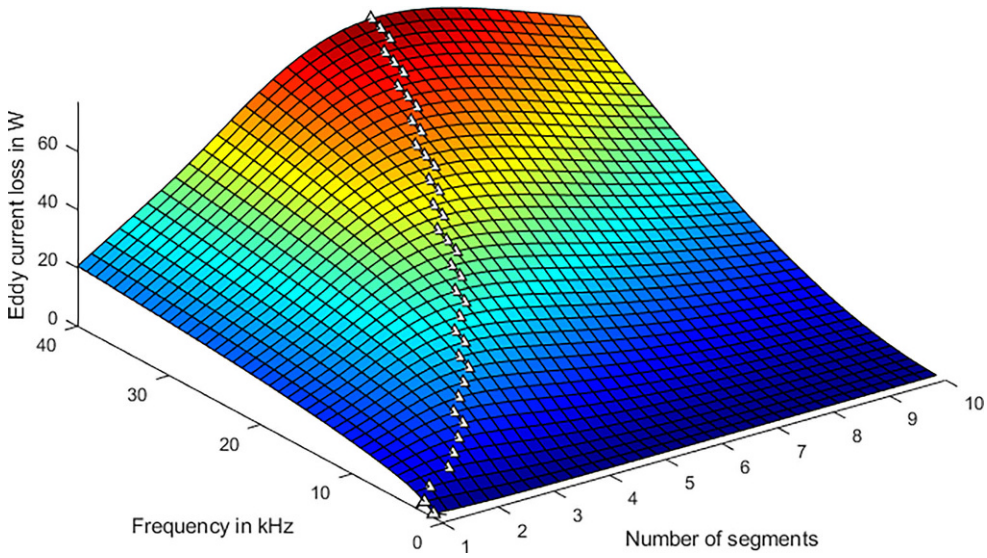

Fig. 7 Current impressed eddy current losses for various frequencies and number of segments

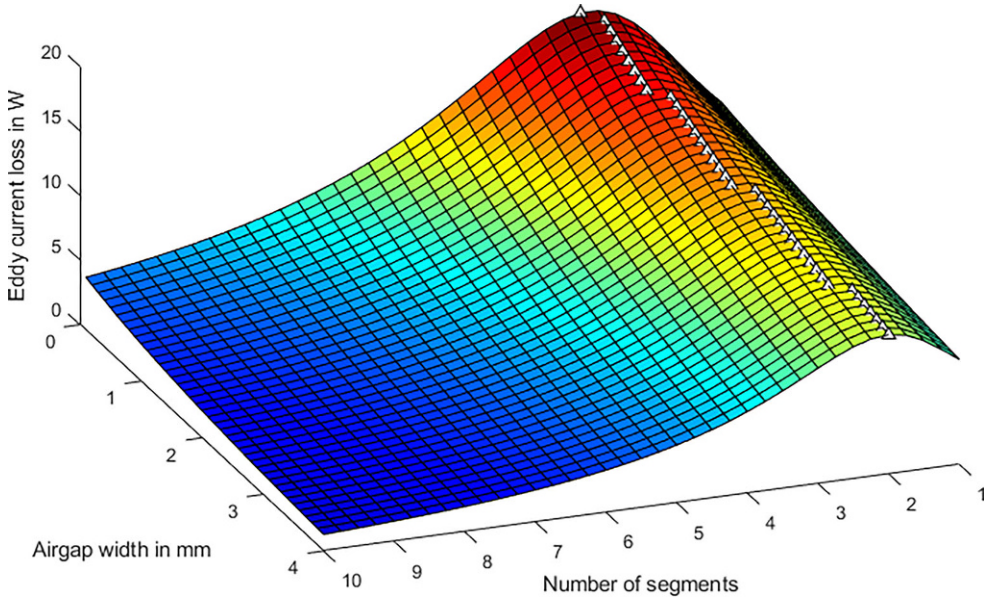

Fig. 8 Eddy current losses for various air gap widths and number of segments (current impressed analysis)

reluctance, the PM eddy current losses are reduced as the air gap width is increased.

For embedded permanent magnet synchronous machines the air gap seen by the flux of the permanent magnet is zero. We can model this by adding the leakage factors for all the inductances, since the direct short-circuit for the magnetic flux does not contribute to the reaction flux within the main excitation coil. Fig. 9 shows that higher leakage flux factors (here all three leakage factors are changed simultaneously) increase the inductance of the respective lumped subcircuits. It can also be seen that a higher leakage flux factor requires an increase in the number of segments for an effective PM eddy current loss reduction.

Mostly neglected in conventional PM eddy current loss calculations are the core losses in the ferromagnetic material of the machine (e.g. [2–5]). Since the calculation of core losses is complicated enough the introduction of these losses is simply out of scope for most simulations. However, a strong coupling between core losses and PM eddy current losses is expected. The core losses of the ferromagnetic core create a non-constant inductance as seen from the excitation coil. Both the PM eddy current losses and the core losses create reaction flux effects. Or, in the case of minor hysteresis loop, attenuate the field seen by the PM. The analysis of the hysteresis losses is not done in this paper. However, a simple circuit can be used to estimate the effect of eddy current losses in ferromagnetic materials. The results of the following analysis are shown in Fig. 10. Segmentation increases the eddy current losses in the ferromagnetic material. A high eddy current loss in the ferromagnetic material can have a damping effect on the flux and therefore significantly reduce the losses within the PM. It is important to note that both must be analyzed together.

The effects of reaction flux can be attributed to a power matching problem in the complex plane. The

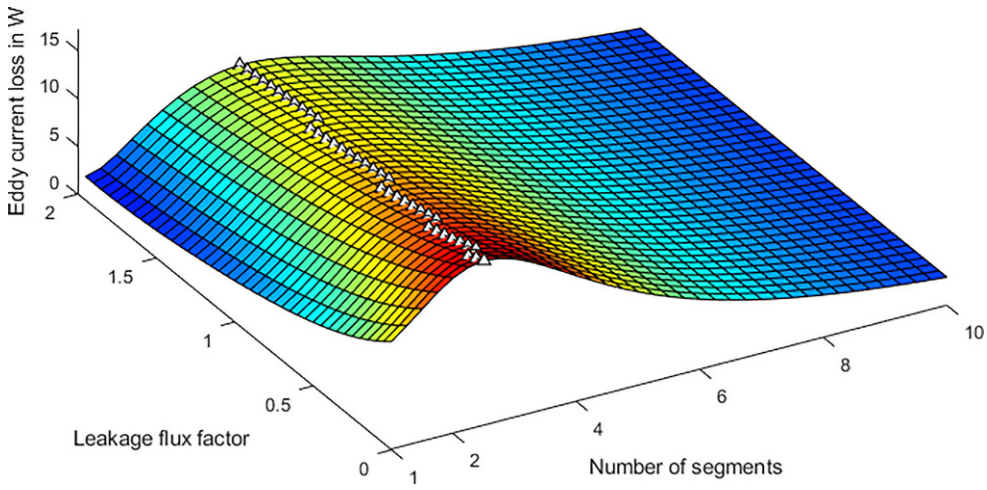

Fig. 9 Eddy current losses for various leakage flux factors and number of segments (current impressed analysis)

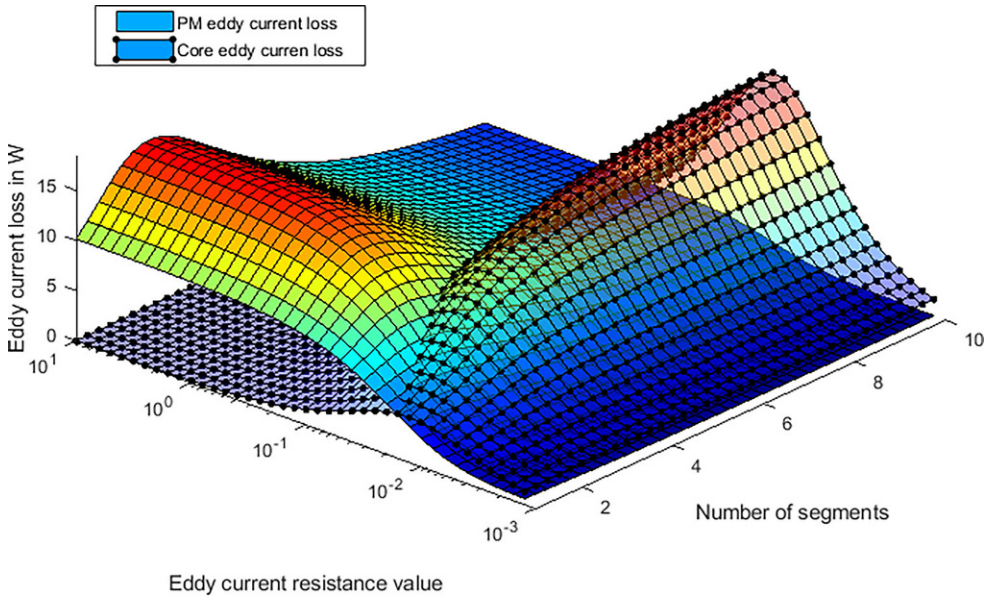

Fig. 10 Eddy current losses for various core eddy current resistances and number of segments (current impressed analysis)

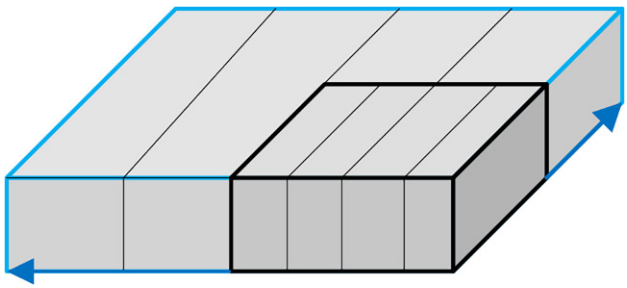

Fig. 11 Magnet size variation for Figs. 12 and 23

maximum power is converted in the sink when the source impedance matches the sink impedance. In complex problems, there are two design choices to limit these losses. Both the reactance and the resistance can be manipulated. Scaling the dimensions of a square permanent magnet equally in length and width changes the ratio of reactance to resistance. The resistance of a given path scales linearly with the scaling factor of the magnet, while the inductance as a function of area scales with the square of the scaling factor of the magnet. The effect on eddy current losses in the PM is shown in Fig. 12. It can be observed that the reaction flux plays are more dominant role in larger magnets. As a result, larger magnets must have a higher number of segments to effectively reduce PM eddy current losses.

Changing the scaling factor of the magnet only in the direction of the segmentation (Fig. 14) does not change the number of segments with the highest losses as much as scaling in both directions (Fig. 12).

Changing only the scaling factor of the magnet orthogonal to the direction of the segmentation (Fig. 16) changes the number of segments where the highest loss occurs similarly to the scaling in both directions (Fig. 12).

In the current impressed case, the number of turns of the excitation coil increases the eddy current losses in the permanent magnet as the flux amplitude increases (Fig. 17). However, a change in the worst case number of segments is observed.

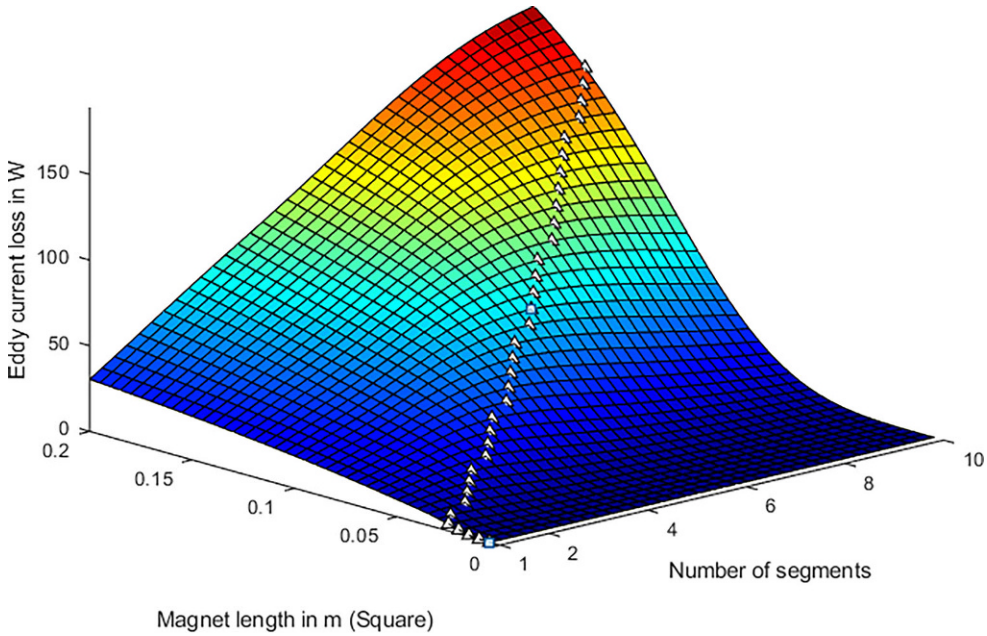

Fig. 12 Eddy current losses for various magnet sizes and number of segments (current impressed analysis)

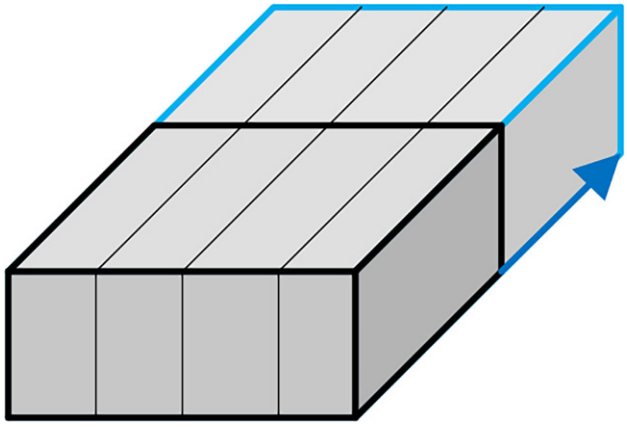

Fig. 13 Magnet size variation for Figs. 14 and 24

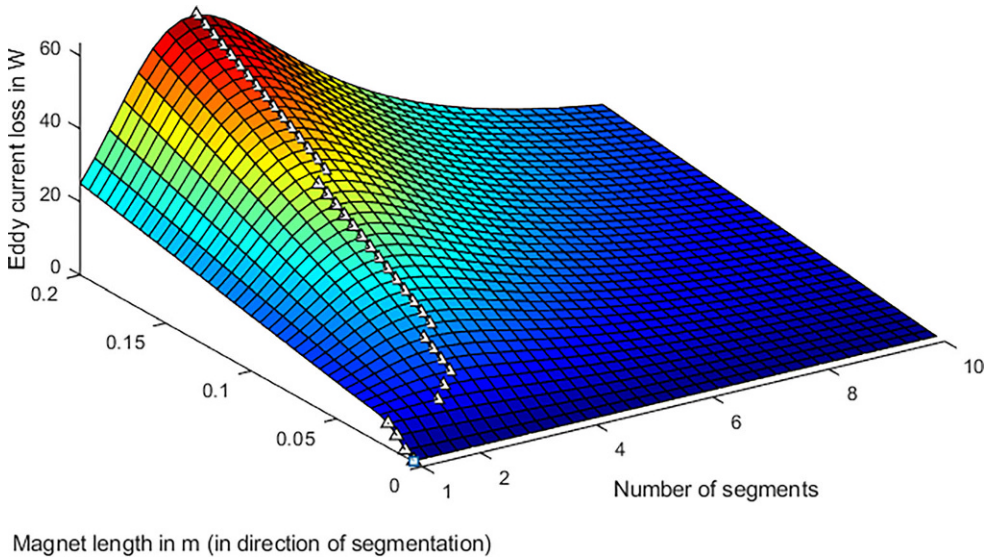

Fig. 14 Eddy current losses for various magnet lengths and number of segments (current impressed analysis)

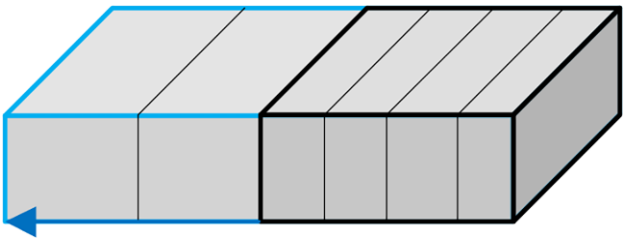

Fig. 15 Magnet size variation for Figs. 16 and 25

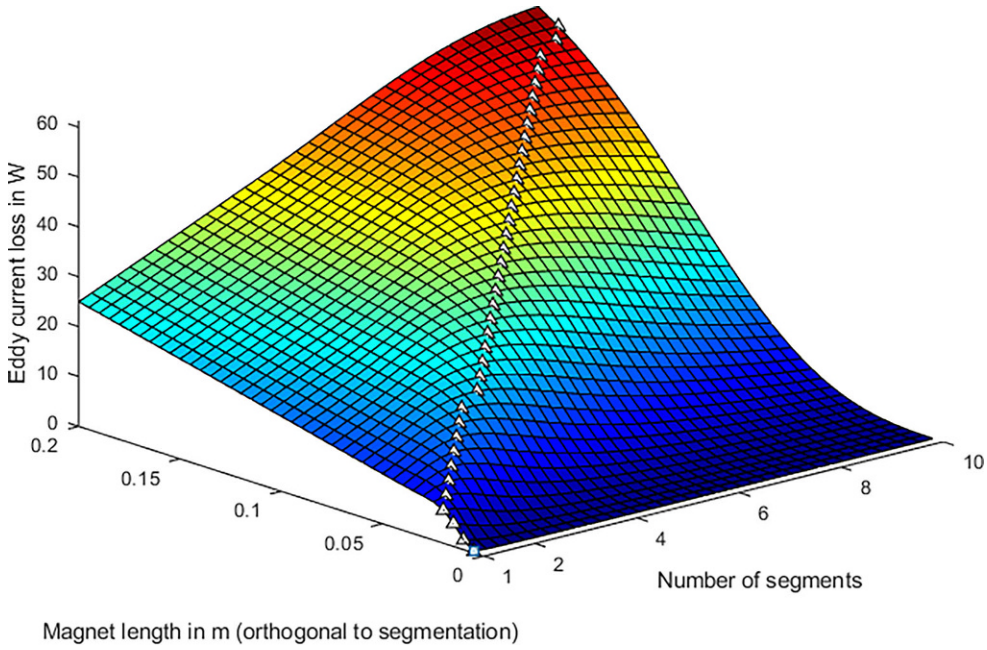

Fig. 16 Eddy current losses for various magnet widths and number of segments (current impressed analysis)

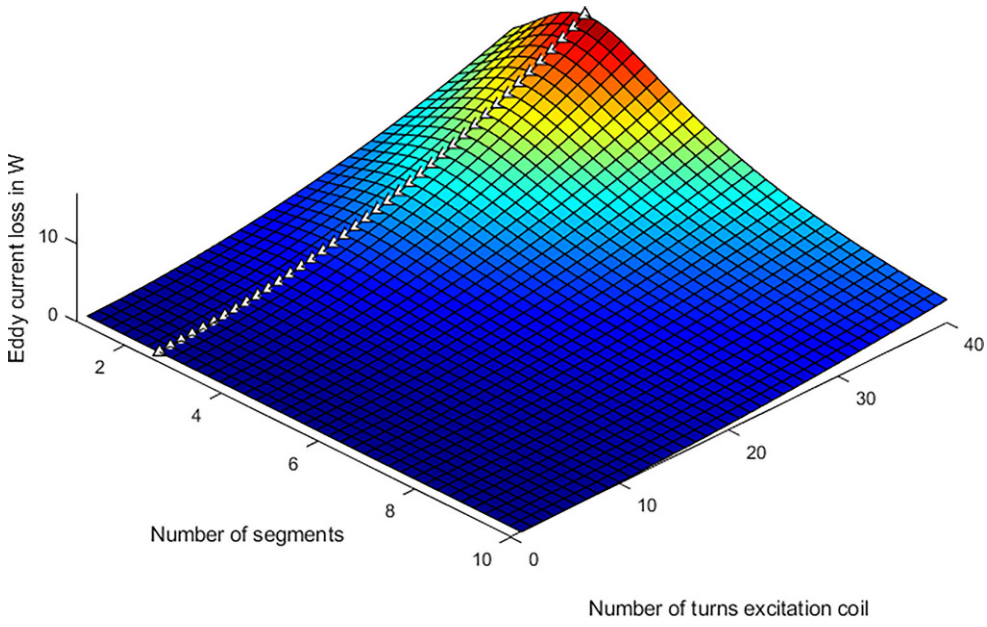

Fig. 17 Eddy current losses for various numbers of coil turns and number of segments (current impressed analysis)

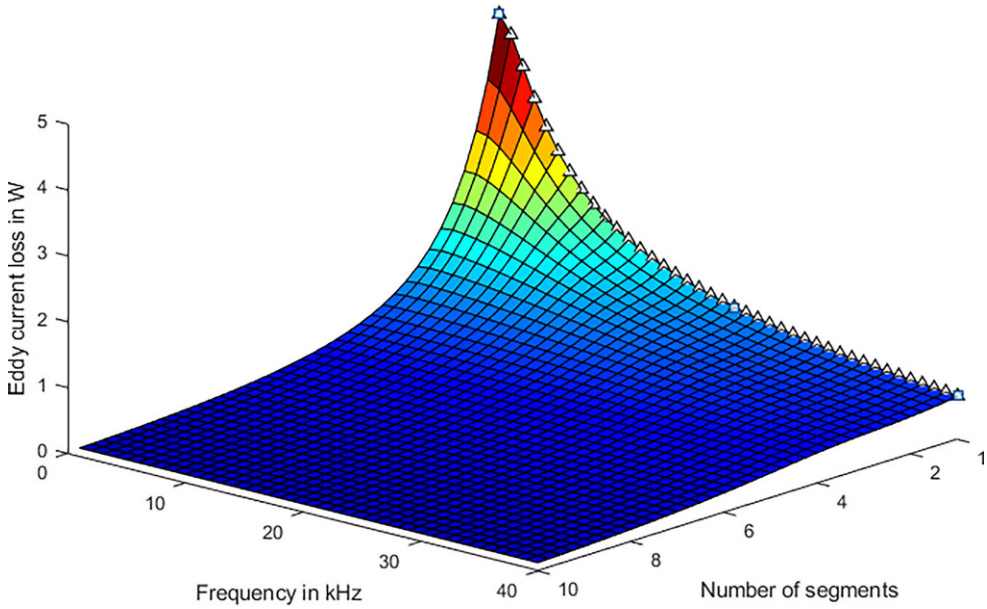

Fig. 18 Eddy current losses for various frequencies and number of segments (voltage impressed analysis)

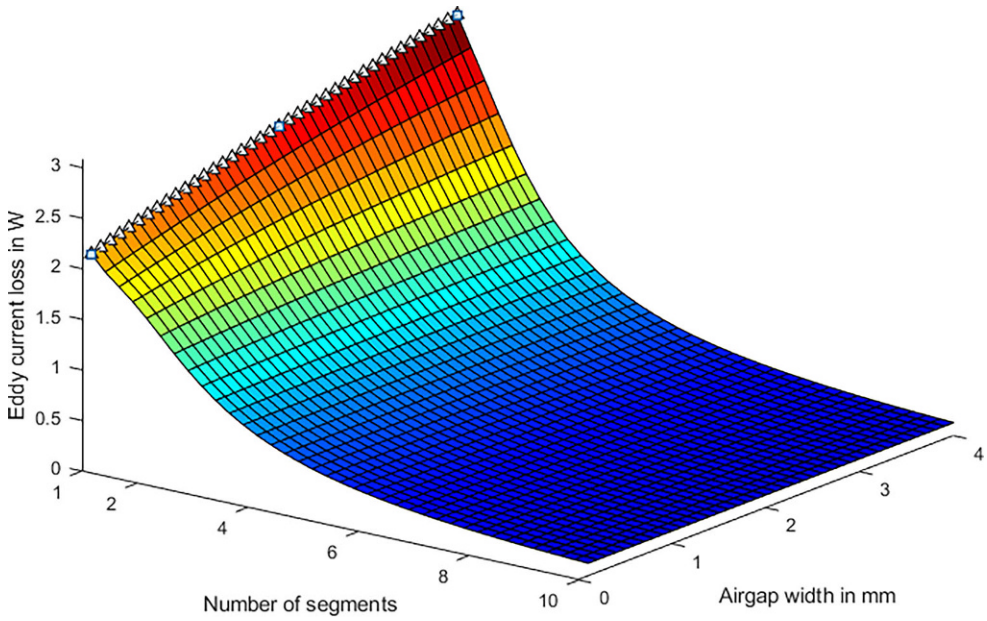

Fig. 19 Eddy current losses for various air gap widths and number of segments (voltage impressed analysis)

4.2 Voltage impressed analysis

The non-constant behavior of the effective excitation coil inductance, and also the reaction flux of the system, changes the behavior between a current impressed and a voltage impressed analysis. In terms of inverter related losses, a voltage impressed analysis seems to be the more accurate choice. Inverter current ripple is mostly defined by the DC link voltage and is not current impressed. When comparing the current impressed analysis of the PM eddy current losses in terms of frequency and number of segements Fig. 7 with the voltage impressed analysis, a significant difference is observed. In the voltage impressed analysis, a decrease in eddy current losses can be observed for all frequencies when segmenting the PM. Also, due to the increase in excitation coil reactance, an increase in frequency results in a decrease in eddy current losses in the PM (Fig. 18).

When analyzing the effect of air gap width, the effect on the segmentation effectiveness (Fig. 19) remains similar to Fig. 18. However, compared to the current impressed case where increasing the air gap width decreases the PM eddy current losses, increasing the air gap width for the voltage impressed case increases the PM eddy current losses.

When the flux leakage factor is introduced into the system a change in the eddy current loss behavior is observed. As the leakage factor increases, the eddy current losses no longer decrease monotonically as the number of segments increases (Fig. 20). Note that the lumped model resistance of the excitation coil is

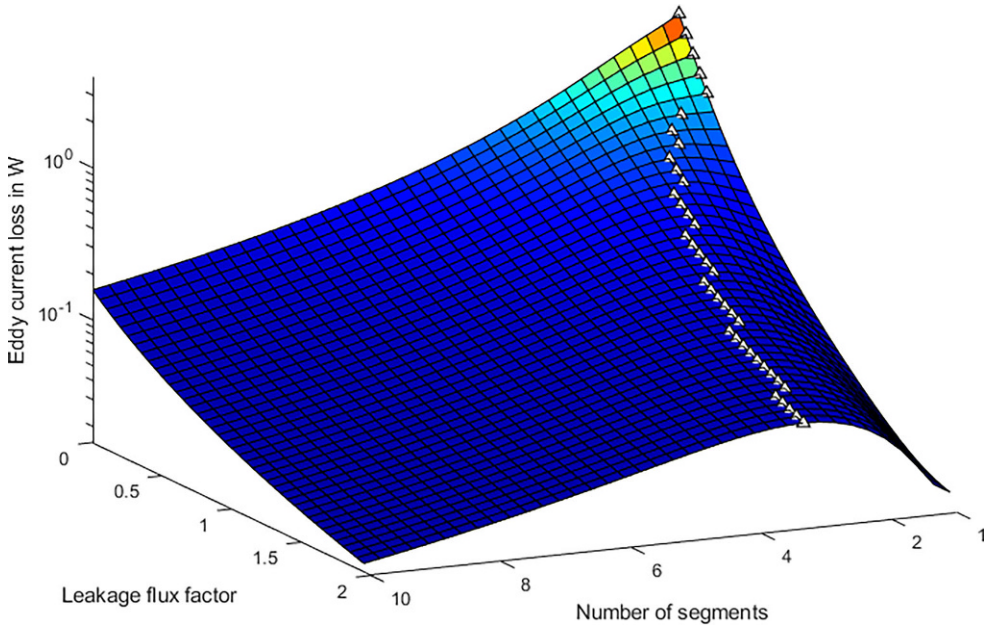

Fig. 20 Eddy current losses for various leakage flux factors and number of segments (voltage impressed analysis)

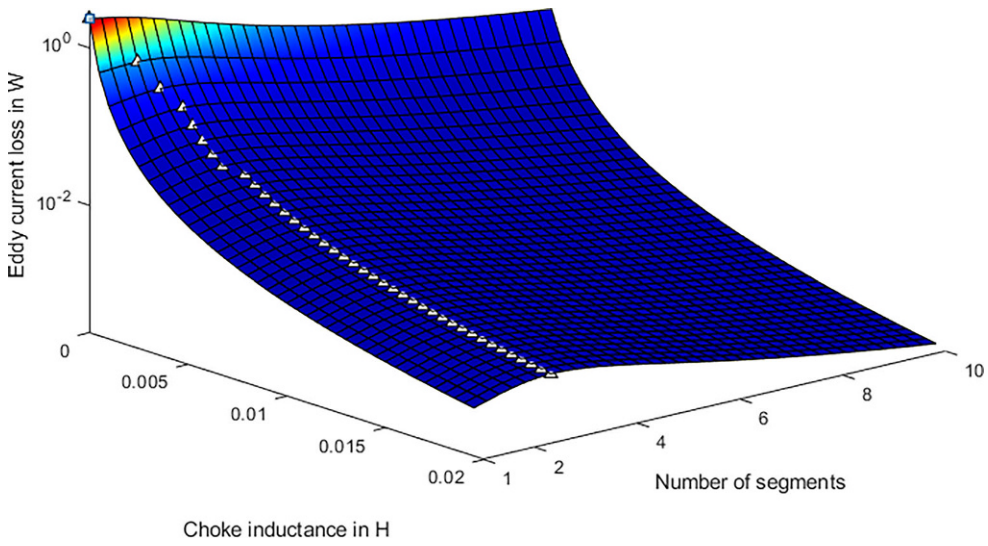

Fig. 21 Eddy current losses for various choke inductance and number of segments (voltage impressed analysis)

modeled as a constant value. As the yoke size increases, another approach would be to increase the resistance as a function of the yoke circumference, which would slightly alter the quantitative results but not the qualitative statements.

A similar effect can be seen when a choke inductance is added to the system (Fig. 21). When a linear reactance is added to the system, the current dependence on the reaction flux and the non-constant system inductance is reduced. As a result, the results shift toward the current impressed case study. Note that a logarithmic scale is used for the eddy current losses in Figs. 21 and 26.

Regarding the effects of the eddy current losses in ferromagnetic materials, a small deviation can still be observed for low eddy current resistances. However, the effects are greatly reduced (Fig. 22). In most cases, the eddy current losses in the ferromagnetic material will be on the side of higher resistivity, since that's the main benefit of electrical steel. If the effective eddy current resistance of the ferromagnetic material is high, the effect on the PM eddy current losses is small.

When changing the size of the permanent magnet by scaling it in both the width and length (Fig. 23). Segmentation reduces PM eddy current losses. As the size of the geometry increases, the inductance also increases as the square of the size, creating a local loss maximum for a given magnet dimension.

Figs. 24 and 25 show the PM eddy current losses for various sizes in the segmentation direction and orthogonal to the segmentation direction, respectively.

One factor that can change the effectiveness of a segmentation in case of voltage impressed analysis is the number of turns in the excitation coil. As the number of turns decreases, a local maximum of eddy

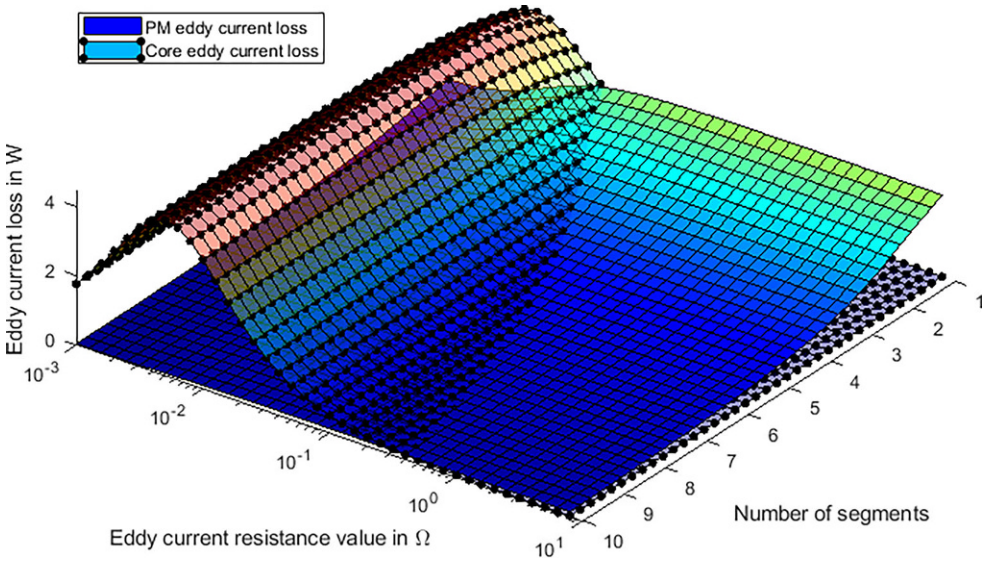

Fig. 22 Eddy current losses for various core eddy current resistances and number of segments (voltage impressed analysis)

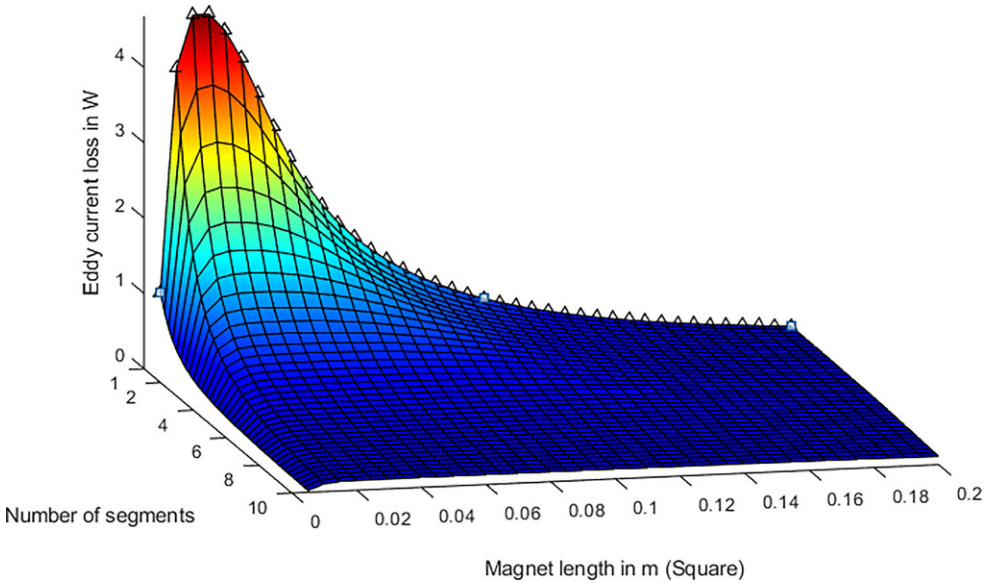

Fig. 23 Eddy current losses for various magnet sizes and number of segments (voltage impressed analysis)

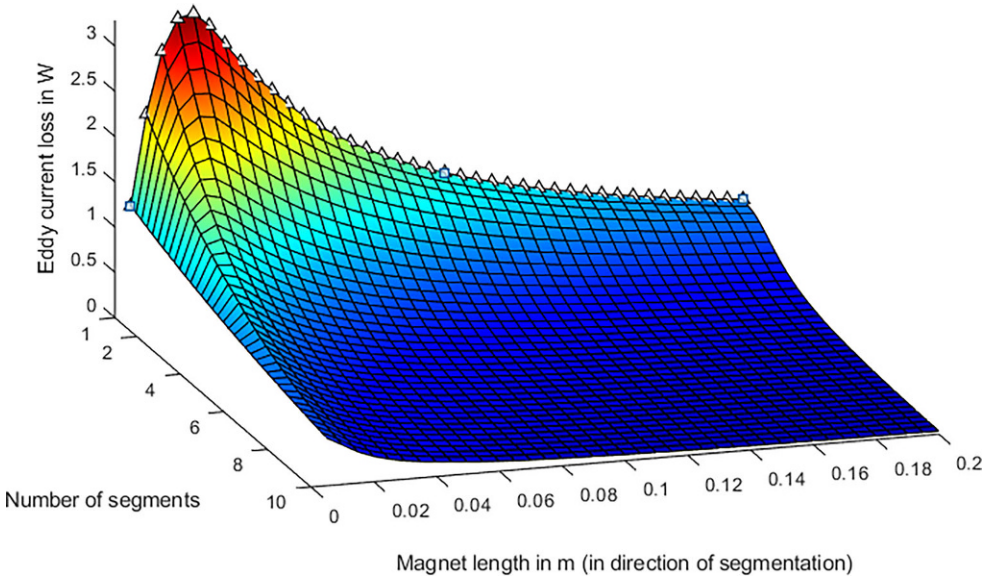

Fig. 24 Eddy current losses for various magnet lengths in the direction of segmentation and number of segements (voltage impressed analysis)

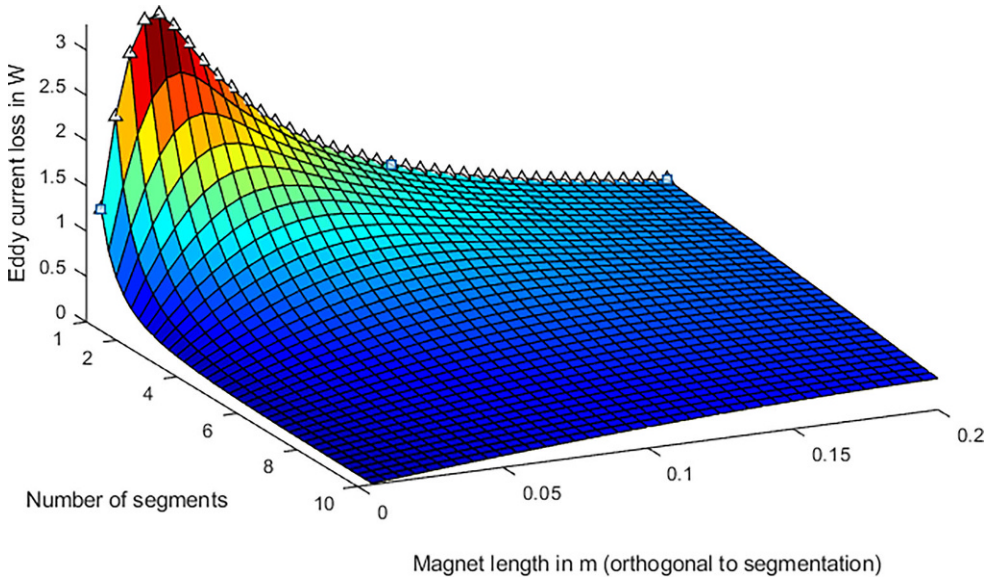

Fig. 25 Eddy current losses for various magnet widths orthogonal to the direction of segmentation and number of segments (voltage impressed analysis)

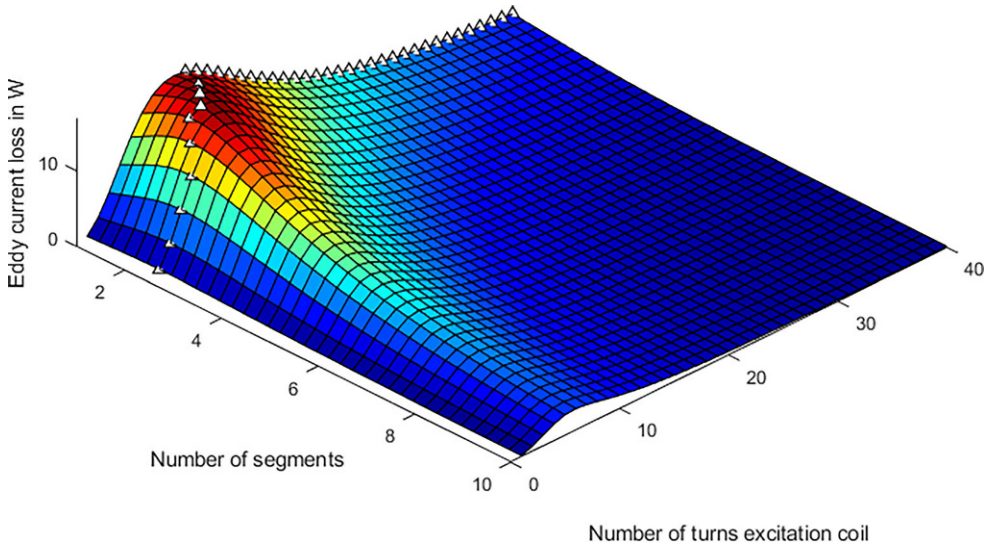

Fig. 26 Eddy current losses for various number of coil turns and number of segments (voltage impressed analysis)

current losses can be observed for a certain number of segments (Fig. 26). Note that the lumped model resistance of the excitation coil is modeled as a constant value according to Table 1. As the number of turns increases, another approach would be to increase the resistance as a function that scales linearly with the number of turns for a constant wire diameter or approximately with the square of the number of turns for a constant winding cross-section.

5 Factors of influence on PM segmentation effectiveness

In Section 4, the factors influencing PM eddy current losses were discussed. All figures include segmentation. For further analysis of the effectiveness of PM segmentation on eddy current losses, a simplified normalized analysis is given below. The PM eddy current losses for an unsegmented magnet based on Table 2 is given as a baseline so the different setups can be compared to each other. It has been found that the current impressed analysis can be very different from the voltage impressed analysis. By adding a choke inductance to the excitation coil, a voltage impressed system can be converted to a current impressed system as shown in Fig. 27. A high leakage flux factor should produce similar results.

Since current and voltage impressed analysis cases can be very different, both analyses will be given consistently in this chapter. Figs. 28 and 29 show the effectiveness of segmentation as a function of the source frequency. In the current impressed case (Fig. 28) a significant effect of the frequency on segmentation effectiveness can be observed. At higher frequencies, a larger number of segments is required to induce PM eddy current loss reduction. In the voltage impressed case Fig. 29, this effect is drastically reduced, but still significant.

The same observation applies to the analysis of different air gap widths (Figs. 30 and 31). Although the

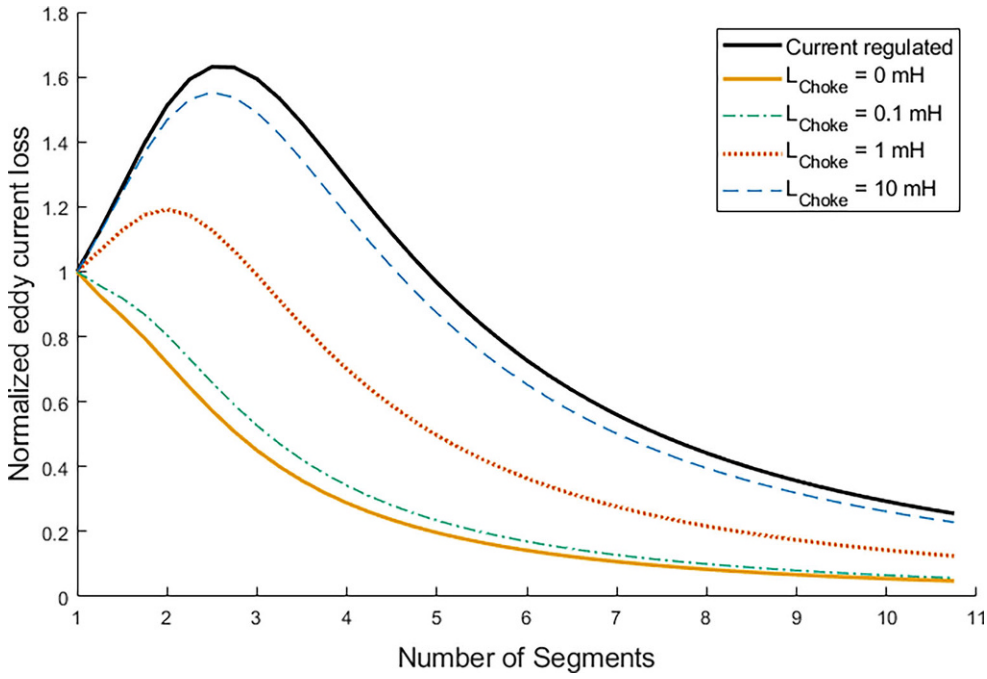

Fig. 27 Influence of choke inductance on PM segmentation effectiveness(voltage impressed analysis)

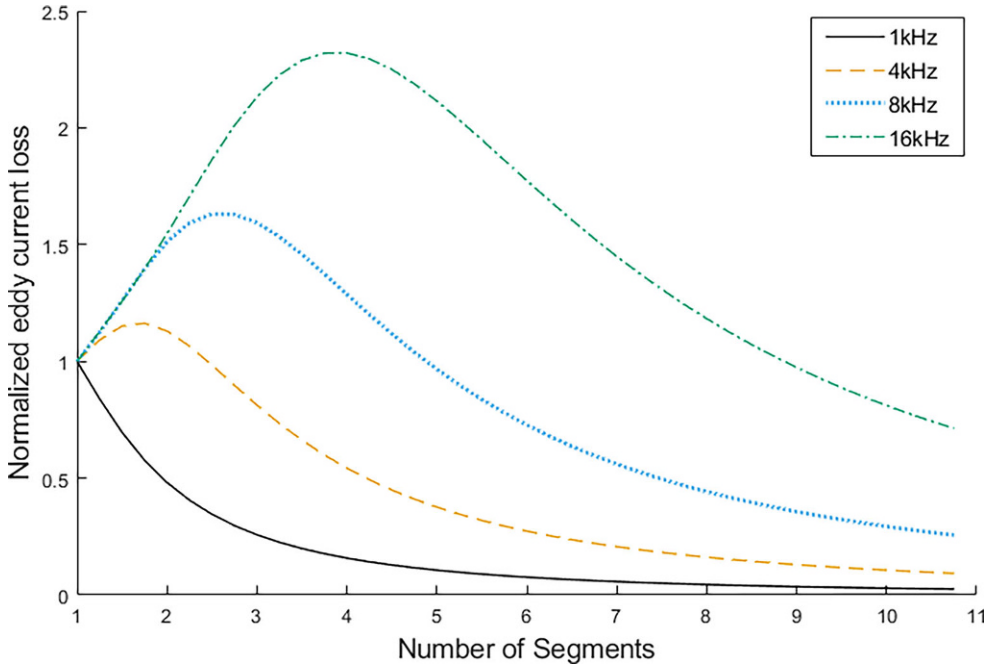

Fig. 28 Influence of inverter switching frequency on PM segmentation effectiveness (current impressed analysis)

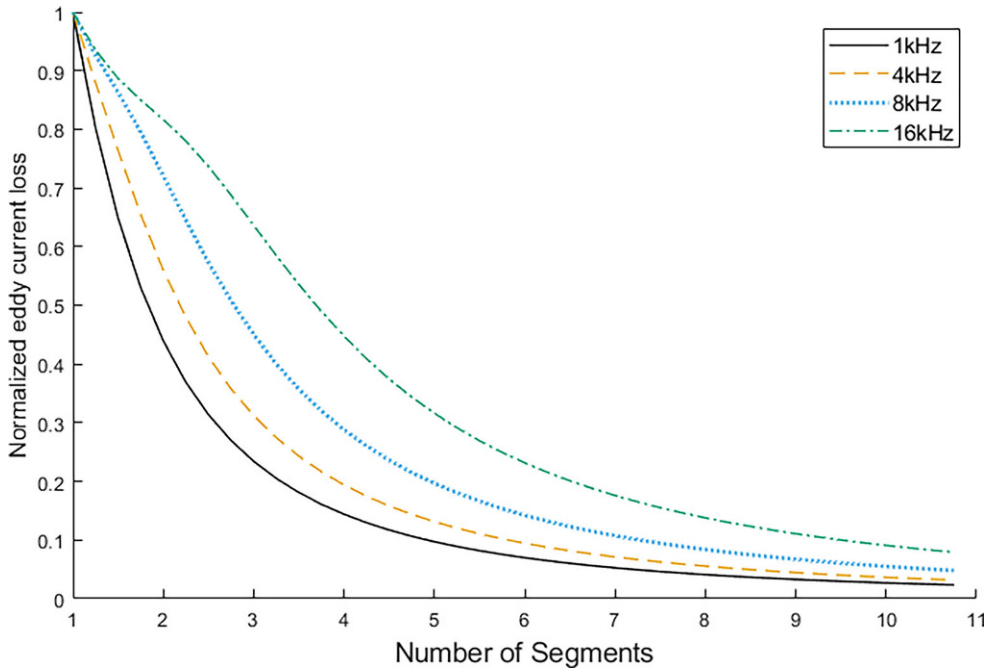

Fig. 29 Influence of inverter switching frequency on PM segmentation effectiveness (voltage impressed analysis)

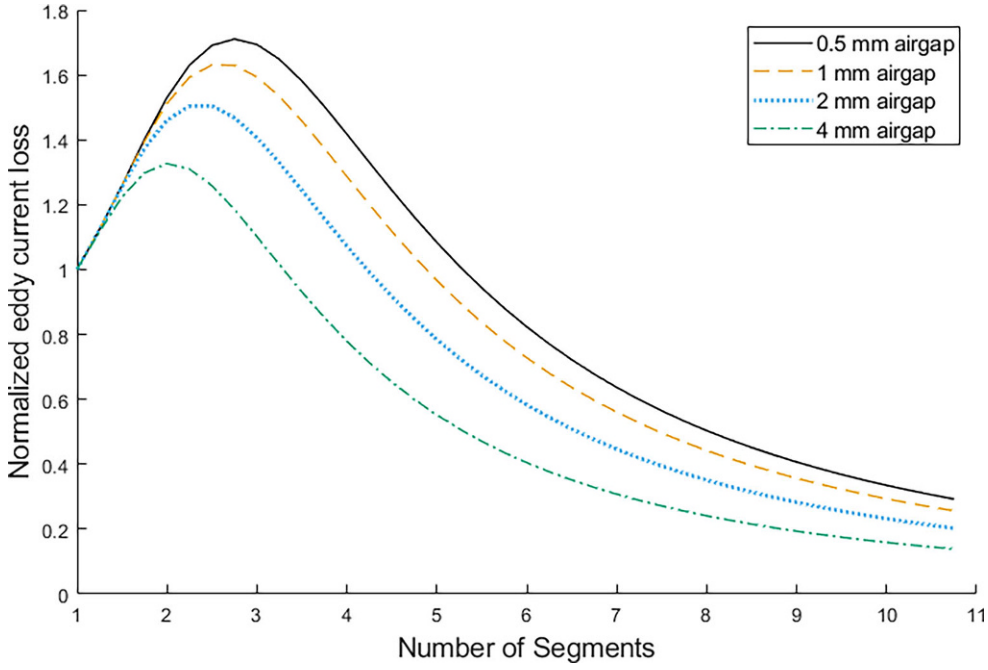

Fig. 30 Influence of air gap width on PM segmentation effectiveness (current impressed analysis)

effect on the effectivness of PM segmentation is less pronounced.

Segmentation effectiveness for electrical machines can vary widely for alternative lamination cuts. In some applications, it is common to include leakage bridges at the top of the stator teeth, which greatly increase the leakage flux. As shown in Figs. 32 and 33 the effectiveness of a given segmentation is highly dependent on the leakage flux characteristics of the machine. This is also true for the differences between surface-mounted permanent magnet machines (SPM) and integrated permanent magnet machines (IPM).

The influence of eddy current losses in the core material is negligible in the voltage impressed case as shown in Fig. 35. However, it should be noted that with an increase in leakage flux or with a choke inductance, the behavior may tend toward the current impressed case shown in Fig. 34

Varying the number of turns and the winding resistance of the primary excitation coil only makes sense in the voltage impressed case. In the current impressed case, the current through the coil does not depend on the resistance or reactance of the winding. Fig. 36 shows the effect of the number of turns of the primary

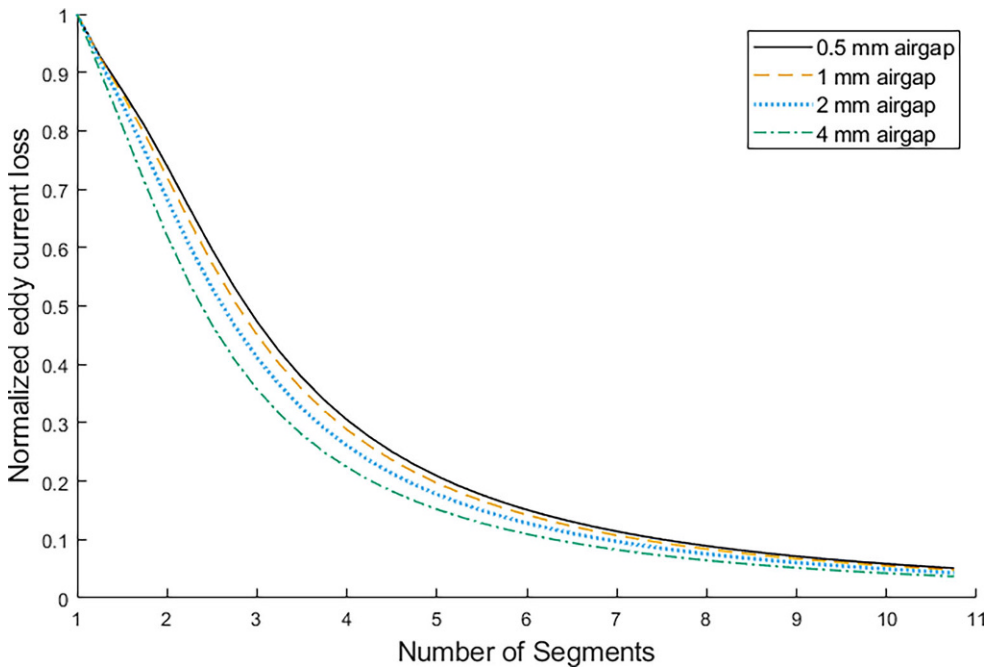

Fig. 31 Influence of air gap width on PM segmentation effectiveness (voltage impressed analysis)

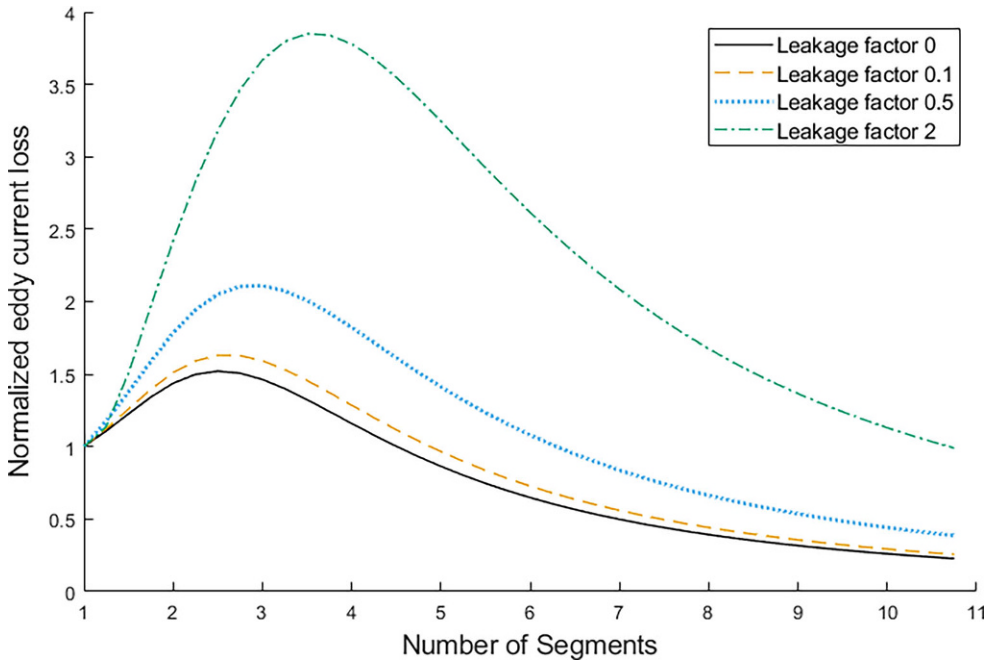

Fig. 32 Influence of leakage flux on PM segmentation effectiveness (current impressed analysis)

coil. A change in segmentation effectiveness can be observed at low turn counts. As the number of turns increases the effectiveness approaches an asymptotic limit. The winding inductance still remains non-constant leading to contrasting results compared to the addition of a choke inductance.

For the same reason in Fig. 27 at top of this section, an increased winding resistance changes the behavior of the voltage impressed system relative to the current impressed system. However, the winding inductance is usually small compared to the inductance.

6 Summary and outlook

An analytical approach to the calculation of PM eddy current losses for homogeneous fields has been given. The analysis of influencing factors on PM eddy current losses can utilize a flux oriented approach, as has been done in several other solution attempts [2, 4, 5]. In addition, a current oriented approach can facilitate eddy current losses within the core of the system being analyzed, which affects the PM eddy current loss and vice versa. This approach is used for winding harmonics in electrical machines. However,for the calculation

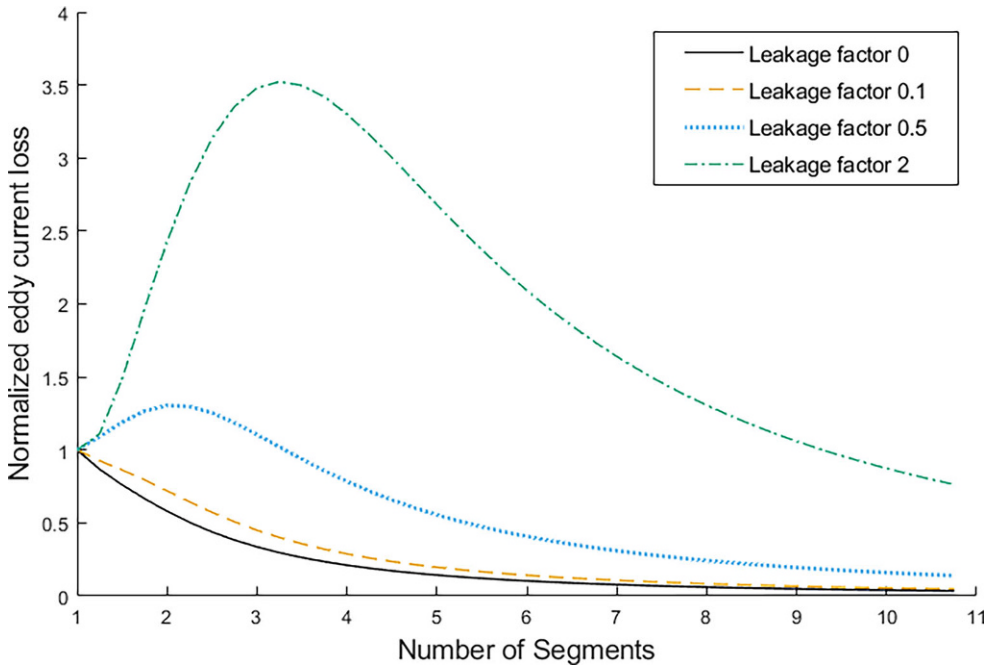

Fig. 33 Influence of leakage flux on PM segmentation effectiveness (voltage impressed analysis)

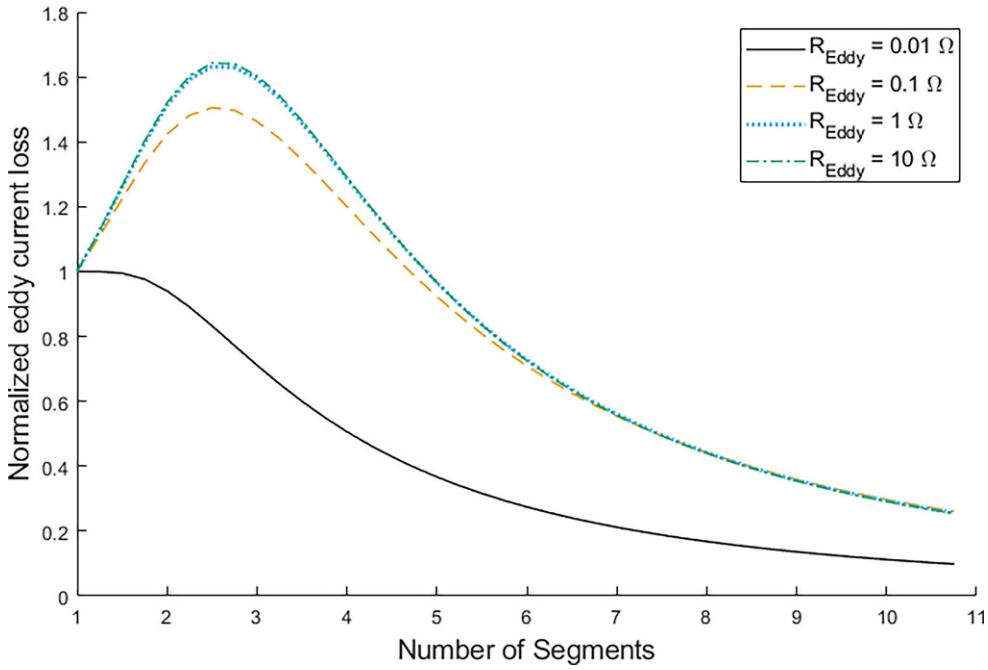

Fig. 34 Influence of effective core eddy current resistance on PM segmentation effectiveness (current impressed analysis)

of inverter related losses, a voltage oriented approach is advantageous. The loss behavior, influencing factors and effectiveness of PM segmentation can vary greatly depending on the approach chosen. Identified significant influence factors on PM segmentation effectiveness include frequency, air gap width, eddy current losses in the near environment for current fixed systems, flux leakage behavior and the number of turns of the primary excitation winding for the voltage fixed system. A large winding resistance or choke inductance can change a voltage fixed system towards a current fixed system and therefore change the segmentation effectiveness. A comprehensive review of the factors influencing segmentation effectiveness is given in Table 3. It is likely that hysteresis of the core material in the vicinity of the magnet alters the effectiveness as well as that hysteresis adds a non linear damping effect to the magnetic fields. This is a topic for further research as it requires a transient model of the hysteresis subloops. Compared to real machines the model is simplified in order to make qualitative statements about the influencing factors on EC losses and segmentation effectiveness. These qualitative effects translate well to real machines. In addition, pre-

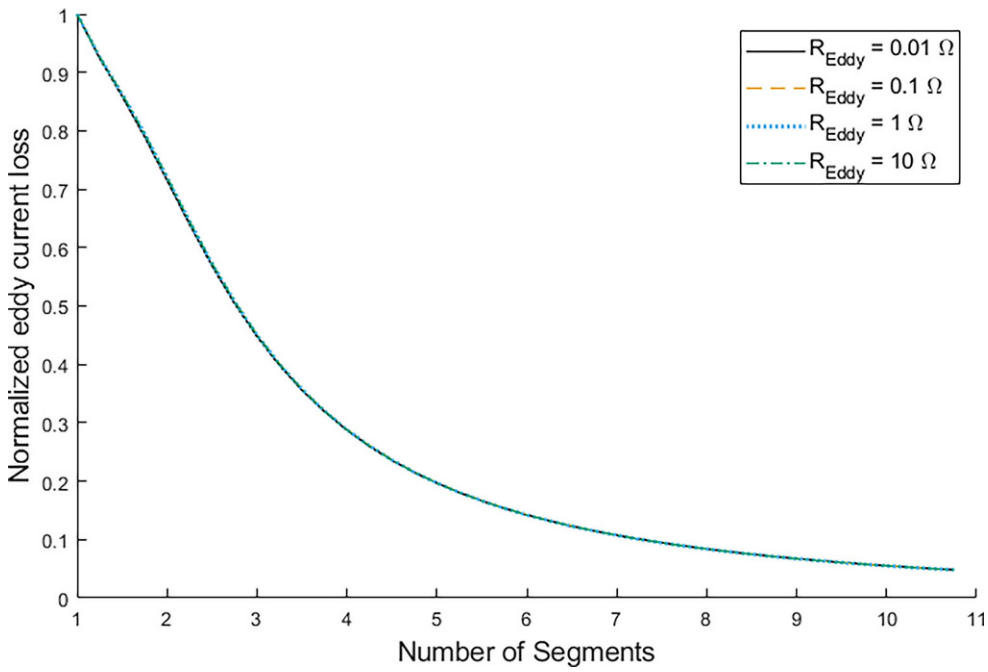

Fig. 35 Influence of effective core eddy current resistance on PM segmentation effectiveness (voltage impressed analysis)

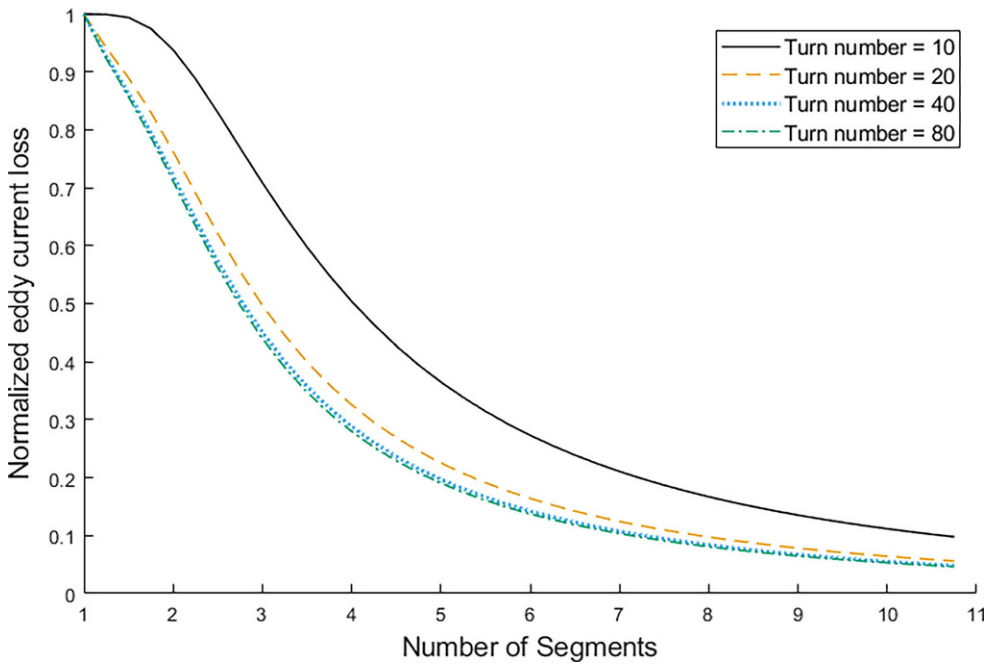

Fig. 36 Influence of the number of turns in the excitation coil on PM segmentation effectiveness (voltage impressed analysis)

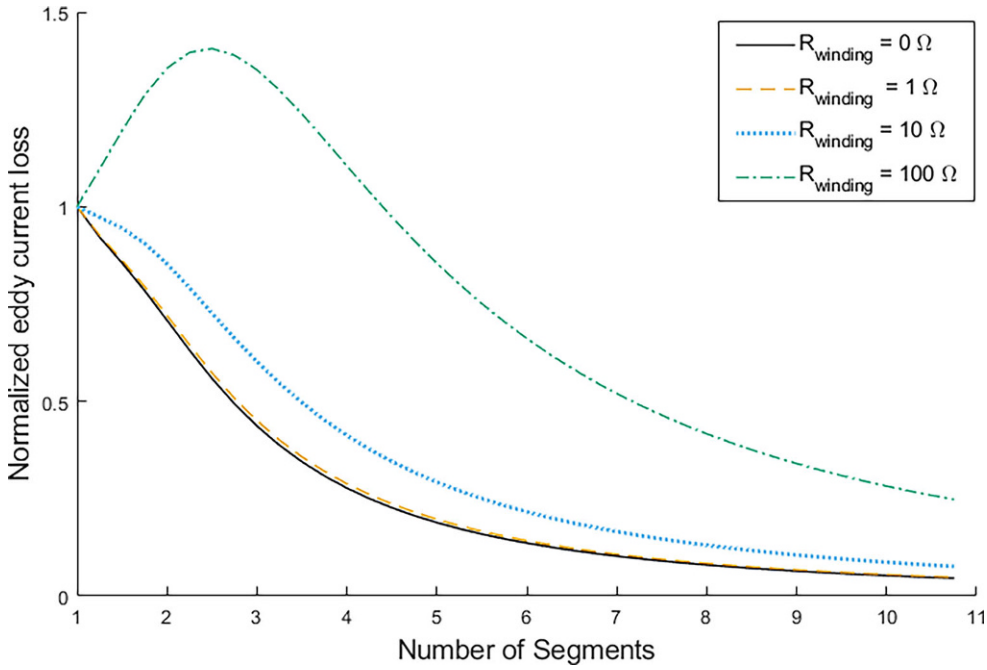

Fig. 37 Influence of excitation coil resistance on PM segmentation effectiveness (voltage impressed analysis)

Table 3 Summary of influence parameters

Influence factor	Current impressed analysis	Voltage impressed analysis
Frequency	High	Moderate
Air gap width	High	Low
Flux leakage	High	High
Choke inductance	None	High
Eddy currents in	Moderate	Very low
Ferromagnetic material		
Magnet dimension	High	Low
Orthogonal & parallel		
Magnet dimension	Moderate	Low
Orthogonal		
Magnet dimension	High	Low
Parallel		
Coil turn number	None	Low
Coil resistance	None	Moderate

liminary results have shown that the model works well for fast approximation of inverter-related eddy current losses in PM, which is the subject of ongoing research. For slot and winding harmonics, however, the model is poorly equipped and should not be used to make qualitative statements.

Funding Open Access funding enabled and organized by Projekt DEAL.

References

1. S. Ruoho, T. Santa-Nokki, J. Kolehmainen and A. Arkkio, "Modeling Magnet Length In 2-D Finite-Element Analysis of Electric Machines," in IEEE Transactions on Magnetics, vol. 45, no. 8, pp. 3114–3120, Aug. 2009, https://doi.org/10.1109/TMAG.2009.2018621.
2. K. Yamazaki, M. Shina, Y. Kanou, M. Miwa and J. Hagiwara, "Effect of Eddy Current Loss Reduction by Segmentation of Magnets in Synchronous Motors: Difference Between Interior and Surface Types," in IEEE Transactions on Magnetics, vol. 45, no. 10, pp. 4756–4759, Oct. 2009, https://doi.org/10.1109/TMAG.2009.2024159.
3. J. D. Ede, K. Atallah, G. W. Jewell, J. B. Wang and D. Howe, "Effect of Axial Segmentation of Permanent Magnets on Rotor Loss in Modular Permanent-Magnet Brushless Machines," in IEEE Transactions on Industry Applications, vol. 43, no. 5, pp. 1207–1213, Sept.-oct. 2007, https://doi.org/10.1109/TIA.2007.904397.
4. R. Sahu, P. Pellerey and K. Laskaris, "Eddy Current Loss Model Unifying the Effects of Reaction Field and Non-Homogeneous 3-D Magnetic Field," in IEEE Transactions on Magnetics, vol. 56, no. 2, pp. 1–4, Feb. 2020, Art no. 7508404, https://doi.org/10.1109/TMAG.2019.2953110.
5. M. Hullmann and B. Ponick, "General Analytical Description of the Effects of Segmentation on Eddy Current Losses in Rectangular Magnets" ICEM 2022, https://doi.org/10.1109/ICEM51905.2022.9910629
6. G. Bertotti, "Hysteresis in Magnetism", 1st Edition, Academic Press, May 1998, ISBN: 9780120932702
7. M. Koenigs and B. Loehlein, "Lumped model for the calculation of harmonic eddy current loss in permanent magnets for homogeneous flux distributions considering eddy cur-

rent reaction flux", https://doi.org/10.1007/s00502-023-01147-z

Mike Königs, received his B.Eng. in electrical engineering from the Frankfurt University of Applied Sciences, Germany in 2017 where he enrolled in a dual course of study with the Siemens AG. In 2019 he received his M.Sc. in electrical engineering from the Technical University Kaiserslautern, Germany. After one year in the Test Center Drives with SEW Eurodrive in Bruchsal, Germany he started to work as scientific staff member at the Flensburg University of Applied Sciences where he is pursuing his Ph.D.

Bernd Löhlein, received his diploma in electrical engineering and information technology from the Technical University Kaiserslautern, Germany in 2007. He completed his doctorate in 2012 and after another six years his habilitation on materials in electrical engineering and mechatronic systems with permanent magnet excited synchronous machines. 2018 he headed the Chair of Mechatronics and Electrical Drive Systems for one year as a deputy professor. In 2019, Bernd Löhlein became full professor for electrical drive technology at University of Applied Sciences, Flensburg. In 2020 he founded the research group for Innovative Drive Technology in Flensburg. Since 2020, Bernd Löhlein is also external lecturer at Kiel University for electric drives.